

Analog SC-FDE using Single Sideband Technique

Thanh Hai VO[†] Shinya KUMAGAI[†] and Fumiyuki ADACHI[‡]

Department of Communications Engineering, Graduate School of Engineering, Tohoku University
6-6-05 Aza-Aoba, Aramaki, Aoba-ku, Sendai, Miyagi, 980-8579 Japan

[†]{vothanhai, kumagai}@mobile.ecei.tohoku.ac.jp, [‡]adachi@ecei.tohoku.ac.jp

Abstract—In order to improve performance of analog signal transmission, we recently proposed a novel analog single-carrier transmission with frequency-domain equalization (analog SC-FDE). Analog SC-FDE adopts double sideband (DSB) technique (referred to as analog SC-DSB-FDE) to transmit signal. In this paper, in order to double the spectrum efficiency of analog SC-DSB-FDE, single sideband (SSB) technique is introduced. Analog SC-SSB-FDE applies discrete Fourier transform (DFT), frequency-domain spectrum shaping filter and mapping, inverse DFT (IDFT), and cyclic prefix (CP) insertion before transmission. At the receiver, one-tap FDE is applied to take advantage of frequency diversity and a spectrum copy for restoring spectrum is applied. By computer simulation, we show that analog SC-SSB-FDE achieves better normalized mean square error (NMSE) performance than conventional analog SSB transmission and keeps the performance quality similar to analog SC-DSB-FDE.

Keywords—*analog signal transmission; frequency-domain equalization; single sideband*

I. INTRODUCTION

Nowadays, although digital signal transmission has been continuously evolving [1], analog signal transmission (e.g., radio broadcasting) still remains essential. In comparison with digital signal transmission, a narrower occupied bandwidth is achieved in analog signal transmission since it does not need any source coding nor channel coding. In other words, analog signal transmission has much higher spectrum efficiency than digital signal transmission. However, because of the narrowband transmission, the channel in analog signal transmission is considered as frequency-nonselective fading channel [2]. As consequence of suffering from the frequency-nonselective fading channel, the received signal power drops over a consecutive period of time and hence, the received signal quality degrades seriously. In order to overcome this problem, we recently proposed a novel analog single-carrier transmission with frequency-domain equalization (analog SC-FDE) [3]. The proposed analog SC-FDE adopts a double sideband (DSB) technique to transmit analog signal. Therefore, we call the previously proposed scheme as analog SC-DSB-FDE to easily differentiate from a novel transmission technique in this paper. Analog SC-DSB-FDE widens the bandwidth of analog signal by using discrete Fourier transform (DFT) and mapping the frequency components over a much broader bandwidth. At the receiver, one-tap FDE [4]-[6] is applied to take advantage of frequency-selective fading channel (i.e., frequency diversity). Multi-access in analog SC-DSB-FDE is also possible based on the principle of frequency-division multiple access (FDMA) [7]. Therefore, the spectrum

efficiency is the same as conventional analog signal transmission, inherently narrowband. We showed that analog SC-DSB-FDE achieves better normalized mean square error (NMSE) performance than conventional analog signal transmission while keeping high spectrum efficiency. In particular, combining distributed mapping and minimum mean square error (MMSE) equalization gives the best performance [3].

However, because the frequency spectrum of analog SC signal has a complex conjugate relation between upper sideband (USB) and lower sideband (LSB), the whole spectrum can be reproduced from one of these sidebands. In this paper, in order to double the spectrum efficiency of analog SC-DSB-FDE, we introduce a single sideband (SSB) transmission into analog SC-DSB-FDE and refer to the novel scheme in this paper as analog SC-SSB-FDE. It should be noted that analog SC-FDE includes both analog SC-DSB-FDE and analog SC-SSB-FDE.

Analog SC-SSB-FDE applies DFT, frequency-domain spectrum shaping filter and mapping, inverse DFT (IDFT), and cyclic prefix (CP) insertion before transmission. At the receiver, in addition to applying one-tap FDE, a spectrum copy is implemented to reproduce the original signal spectrum. By computer simulation, we show that analog SC-SSB-FDE achieves better NMSE performance than conventional analog SSB transmission and keeps the performance quality similar to analog SC-DSB-FDE. The remainder of this paper is organized as follows. In section II, we propose the system model of analog SC-SSB-FDE and describe the principle. Computer simulation results are given in Section III. Then, Section IV provides the conclusion.

II. ANALOG SC-SSB-FDE

A. System Model

The system model of analog SC-SSB-FDE is shown in Fig. 1. At the transmitter, after the signal bandwidth is limited by low-pass filter (LPF), the analog signal $s(t)$ is sampled at the Nyquist rate. Then, the sample sequence is grouped into a sequence of signal blocks of M samples each. Each signal block $\{s(n); n=0\sim M-1\}$ is transformed by M -point DFT into frequency-domain signal block $\{S(k); k=0\sim M-1\}$. Spectrum shaping filter is designed to remove the frequency components in USB or LSB. In this paper, each frequency component is referred to as a subcarrier and the removal of USB is considered. The resultant subcarriers $\{\hat{S}(k); k=0\sim M/2\}$ are mapped over a broad bandwidth having N_c ($>M$) orthogonal

subcarriers with zeros occupying the unused subcarriers. Then, the resultant N_c subcarriers are transformed by N_c -point IDFT back into complex time-domain signal block $\{x(n); n=0 \sim N_c-1\}$. Finally, the last N_g samples of the complex time-domain signal block are copied as a CP and inserted into the guard interval (GI) placed at the beginning of each transmit signal block.

The CP-inserted signal block is transmitted over a frequency-selective fading channel. At the receiver, CP is removed from each received signal block and then, each block is transformed by N_c -point DFT into N_c subcarrier components. After performing de-mapping and FDE, M subcarriers of original signal are restored by the spectrum copy and transformed by M -point IDFT back into complex signal block $\{\tilde{s}(n); n=0 \sim M-1\}$ of M samples. Finally, the analog signal $\tilde{s}(t)$ is reconstructed after applying the automatic gain control (AGC) [8] and LPF.

B. Transmit Signal Representation

At the transmitter, the frequency components after M -point DFT $\{S(k); k=0 \sim M-1\}$ are inputted to the spectrum shaping filter which is assumed to be an ideal brick wall LPF in this paper. The frequency components (referred to as subcarriers) in USB, which have the complex conjugate relation with that in LSB shown in Fig. 2, are removed. Therefore, the output includes only the subcarriers in LSB which are denoted by $\{\hat{S}(k); k=0 \sim M/2\}$ and expressed as

$$\hat{S}(k) = \sqrt{Q} \times \frac{1}{\sqrt{M}} \sum_{n=0}^{M-1} s(n) \exp\left(-j2\pi k \frac{n}{M}\right), \quad (1)$$

where $\sqrt{Q} = \sqrt{M/(M/2+1)}$ is a normalization factor to keep the total signal power the same as in analog SC-DSB-FDE.

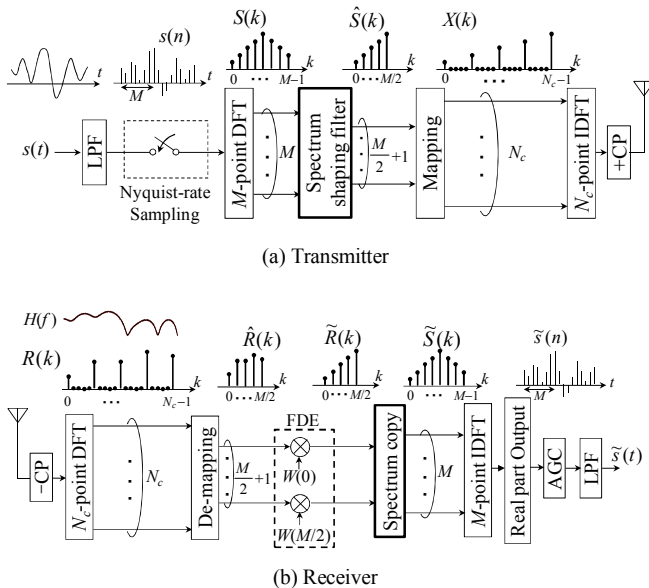


Fig. 1. System model.

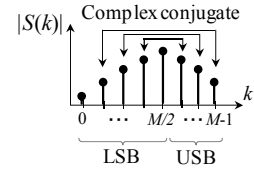


Fig. 2. Frequency components of the analog signal.

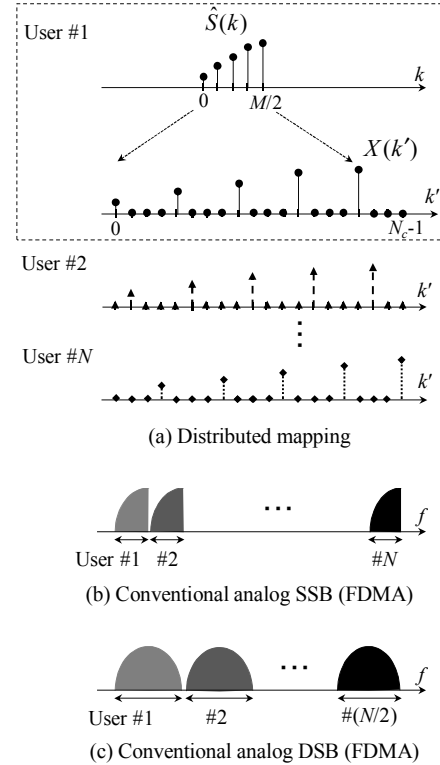


Fig. 3. Subcarrier mapping in proposed analog SC-SSB-FDE and frequency allocation in conventional analog SSB/DSB in accordance with FDMA.

The transmitter then maps the resultant subcarriers $\{\hat{S}(k); k=0 \sim M/2\}$ over a broad bandwidth having N_c ($>M$) orthogonal subcarriers expressed as $\{X(k'); k'=0 \sim N_c-1\}$ in accordance with distributed mapping [7]

$$X(k') = \begin{cases} \hat{S}(k) & , k' = k \times \frac{N_c}{M/2+1} \\ 0 & , \text{otherwise} \end{cases}, \quad (2)$$

where $k'=0 \sim N_c-1$, $k=0 \sim M/2$, and $N_c/(M/2+1)$ is the adjacent original subcarrier interval. The subcarrier mapping is shown in Fig. 3. Because of the equally-spaced subcarrier mapping in which zeros occupy the unused subcarriers, this subcarrier mapping is expected to obtain a significant frequency diversity gain. In case of transmitting multiple analog signal streams, each consisting of M subcarriers, the subcarrier mapping is performed so that original subcarriers of multiple streams do not overlap (or they are orthogonal to each other) in the frequency-domain similar to the principle of FDMA.

After N_c -point IDFT and CP insertion, the time-domain sample sequence $\{\tilde{x}(n); n=-N_g \sim N_c-1\}$ at a rate of

$1/T_s = (N_c/M) \times 1/T$, which $1/T$ is the Nyquist sampling rate of analog signal $s(t)$, can be expressed using the equivalent low-pass representation as

$$\tilde{x}(n) = \sqrt{2P} x(n \bmod N_c), \quad (3)$$

where P is the average sample sequence power and $\{x(n); n = 0 \sim N_c - 1\}$ is given by

$$x(n) = \frac{1}{\sqrt{N_c}} \sum_{k=0}^{N_c-1} X(k) \exp\left(j2\pi n \frac{k}{N_c}\right). \quad (4)$$

C. Received Signal Representation

Assuming that the channel consists of L distinct propagation paths, the channel impulse response $h(\tau, t)$ can be expressed as

$$h(\tau, t) = \sum_{l=0}^{L-1} h_l(t) \delta(\tau - \tau_l), \quad (5)$$

where $h_l(t)$ and τ_l are complex-valued path gain with $E[\sum_{l=0}^{L-1} |h_l(t)|^2] = 1$, ($E[\cdot]$ denotes the expectation operation) and sample-spaced normalized time delay of the l -th path (i.e., $\tau_l = l$), respectively. In (5), we assume that the channel stays constant during the transmission period of one block signal. It is assumed that the maximum time delay of channel is shorter than CP and the received signal is ideally sampled at the rate $1/T_s$. It is assumed that the maximum time delay of channel is shorter than CP length and the received signal is ideally sampled at the rate $1/T_s$. The discrete-time received signal $\{r(n); n = -N_g \sim N_c - 1\}$ is expressed as

$$r(n) = \sum_{l=0}^{L-1} h_l(n) \tilde{x}(n - \tau_l) + \eta(n), \quad (6)$$

where $\eta(n)$ is additive white Gaussian noise (AWGN) with zero-mean and variance $2N_0/T_s$ in which N_0 is the single-side power spectrum density.

After removing CP, each received signal block is transformed by N_c -point DFT into the frequency-domain signal $\{R(k); k=0 \sim N_c-1\}$ which is expressed as

$$R(k) = \sqrt{2P} H(k) X(k) + \Pi(k), \quad (7)$$

where $H(k)$ and $\Pi(k)$ are the channel gain and the noise component at the k -frequency, respectively. They are given by

$$H(k) = H(k, n) = \sum_{l=0}^{L-1} h_l(n) \exp\left(-j2\pi k \frac{\tau_l}{N_c}\right), \quad (8)$$

$$\Pi(k) = \frac{1}{\sqrt{N_c}} \sum_{n=0}^{N_c-1} \eta(n) \exp\left(-j2\pi k \frac{n}{N_c}\right). \quad (9)$$

Then, de-mapping is performed to obtain desired subcarriers $\{\hat{R}(k); k = 0 \sim M/2\}$. Channel gain $\{\hat{H}(k); k = 0 \sim M/2\}$ for FDE and the equivalent noise component $\{\hat{\Pi}(k); k = 0 \sim M/2\}$ are also obtained as follows

$$\begin{cases} \hat{R}(k) = R(k \times N_c / (M/2 + 1)) \\ \hat{H}(k) = H(k \times N_c / (M/2 + 1)), \quad k = 0 \sim M/2. \\ \hat{\Pi}(k) = \Pi(k \times N_c / (M/2 + 1)) \end{cases} \quad (10)$$

After subcarrier de-mapping, one-tap FDE is carried out as

$$\tilde{R}(k) = W(k) \hat{R}(k) = \sqrt{2PW(k)} \hat{H}(k) \hat{S}(k) + W(k) \hat{\Pi}(k), \quad (11)$$

where $\{W(k); k=0 \sim M/2\}$ is the MMSE weight [6] expressed as

$$W(k) = \frac{\hat{H}^*(k)}{|\hat{H}(k)|^2 + (Q\Gamma)^{-1}}. \quad (12)$$

In Eq. (12), $\Gamma = PT_s/N_0$ is the average received signal-to-noise power ratio (SNR) and $[\cdot]^*$ denotes the complex conjugate operation.

The resultant subcarriers $\{\tilde{R}(k); k = 0 \sim M/2\}$ is then used to restore M frequency components $\{\tilde{S}(k); k = 0 \sim M-1\}$ of original analog signal based on the conjugate relation between LSB and USB as

$$\tilde{S}(k) = \begin{cases} \tilde{R}(k) & , \quad k = 0 \sim M/2 \\ \tilde{R}^*(M-k) & , \quad k = M/2+1 \sim M-1 \end{cases}. \quad (13)$$

Next, the resultant M subcarriers $\{\tilde{S}(k); k = 0 \sim M-1\}$ are transformed back into the time-domain signal block by M -point IDFT and only the real part of the time-domain signal $\{\tilde{s}(n); n=0 \sim M-1\}$ is outputted as

$$\begin{aligned} \tilde{s}(n) &= \frac{1}{K} \times \text{Re} \left\{ \frac{1}{\sqrt{M}} \sum_{k=0}^{M-1} \tilde{S}(k) \exp\left(j2\pi n \frac{k}{M}\right) \right\}, \quad (14) \\ &= s(n) + \text{Re} \{ \mu_{\text{ISI}}(n) + \mu_{\text{noise}}(n) \} \end{aligned}$$

where K , $\mu_{\text{ISI}}(n)$, and $\mu_{\text{noise}}(n)$ are normalization factor of AGC, residual signal distortion, and equivalent noise, respectively, which are given by

$$\begin{cases} K = \sqrt{2PQ} \frac{1}{M} \left\{ \sum_{k=0}^{M/2} \tilde{H}(k) + \sum_{k=1}^{M/2-1} \tilde{H}^*(k) \right\} \\ \mu_{\text{ISI}}(n) = \frac{1}{K} \frac{\sqrt{2PQ}}{M} \left\{ \sum_{k=0}^{M/2} \tilde{H}(k) \left[\sum_{\substack{n'=0 \\ n' \neq n}}^{M-1} s(n') \exp\left(j2\pi k \frac{n-n'}{M}\right) \right] \right. \\ \quad \left. + \sum_{k=1}^{M/2-1} \tilde{H}^*(k) \left[\sum_{\substack{n'=0 \\ n' \neq n}}^{M-1} s(n') \exp\left(-j2\pi k \frac{n-n'}{M}\right) \right] \right\}, \\ \mu_{\text{noise}}(n) = \frac{1}{K} \frac{1}{\sqrt{M}} \left\{ \sum_{k=0}^{M/2} \tilde{\Pi}(k) \exp\left(j2\pi n \frac{k}{M}\right) \right. \\ \quad \left. + \sum_{k=1}^{M/2-1} \tilde{\Pi}^*(k) \exp\left(-j2\pi n \frac{k}{M}\right) \right\} \end{cases} \quad (15)$$

in which $\tilde{H}(k) = W(k)\hat{H}(k)$ and $\tilde{\Pi}(k) = W(k)\hat{\Pi}(k)$ being the equivalent channel and the equivalent noise component at the k -th frequency, respectively. Finally, the analog signal $\tilde{s}(t)$ is reconstructed by LPF from discrete signal $\tilde{s}(n)$.

D. Conventional SSB transmission

For comparison, conventional analog SSB transmission [9] is also considered. At the transmitter, the analog signal after applying LPF is modulated to SSB signal by using Hilbert transform, which is assumed to be ideal, before transmission. Due to the narrow bandwidth of signal, we assume that the channel consists of one path (i.e., frequency-nonselective fading channel).

At the receiver, ideal fast AGC suppressing the fluctuation of received signal power due to fading and ideal coherent demodulation are assumed. The continuous-time representation of the SSB demodulated signal $\tilde{s}(t)$ can be expressed as

$$\tilde{s}(t) = s(t) + \text{Re}\left\{\eta(t) / \left(\sqrt{2P} h_0(t)\right)\right\}, \quad (16)$$

where $s(t)$ and $\eta(t)$ are desired signal and the zero-mean complex-valued AWGN having the double-sided power spectrum density $2N_0$, respectively.

III. COMPUTER SIMULATION

In this paper, in order to evaluate transmission performance of the proposed analog SC-SSB-FDE, we use NMSE criterion which is defined by

$$\text{NMSE} = \frac{E[|\tilde{s}(n) - s(n)|^2]}{E[|s(n)|^2]}. \quad (17)$$

TABLE I. COMPUTER SIMULATION CONDITION

Signal transmission	Proposed analog SC-SSB-FDE	Conventional analog SSB
Total no. of subcarriers	$N_c = 8192$	
Time-domain block size	$M = 64$	
No. of channels	$N = 1$	
Spectrum shaping filter	Ideal brick wall LPF	
GI length	$N_g = 16$	
Sampling rate of original analog signal	$1/T = 8 \text{ kHz}$	
Mapping	Distributed	
Hilbert transform		Ideal
Channel	Frequency-selective block Rayleigh fading	Frequency non-selective Rayleigh fading
	$L=16$ -path uniform power delay profile	
FDE weight	MMSE	
Channel estimation & Fast AGC	Ideal	

A. Computer Simulation Condition

The computer simulation condition is summarized in Table I. In the proposed analog SC-SSB-FDE, we assume the bandwidth-restricted (4 kHz) voice transmission. We use a sampling rate $1/T = 8 \text{ kHz}$ for the original analog signal at the transmitter, a time-domain signal block with length of $M=64$ samples, and a bandwidth after subcarrier mapping of $N_c=8192$ subcarriers in which the adjacent subcarrier interval of 125 Hz. The channel is assumed to be a frequency-selective block Rayleigh fading channel having a sample-spaced $L=16$ -path uniform power delay profile. Ideal channel estimation is assumed. On the other hand, in conventional analog SSB transmission, the channel is assumed to be a frequency-nonselective fading channel (i.e. $L=1$ -path Rayleigh fading channel) because of the narrowband signal transmission. Ideal Hilbert transform and fast AGC are also assumed in the conventional analog SSB transmission.

B. NMSE performance

The NMSE performance of the proposed scheme in case of voice transmission is plotted in Fig. 4. For comparison, the performance of conventional analog SSB transmission and analog SC-DSB-FDE are also plotted. It can be seen that the proposed analog SC-SSB-FDE achieves much better performance than conventional analog SSB because the combination of distributed mapping and FDE can take advantage of the channel frequency-selectivity to obtain the significant frequency diversity gain. Additionally, analog SC-SSB-FDE keeps the performance similar to analog SC-DSB-FDE while doubling the spectrum efficiency of analog SC-DSB-FDE owing to the removal of the frequency components in USB before transmission. The reason for the small performance degradation is that the transmitted frequency components of original analog signal is less than that of analog SC-DSB-FDE (i.e., a little smaller frequency diversity gain is obtained).

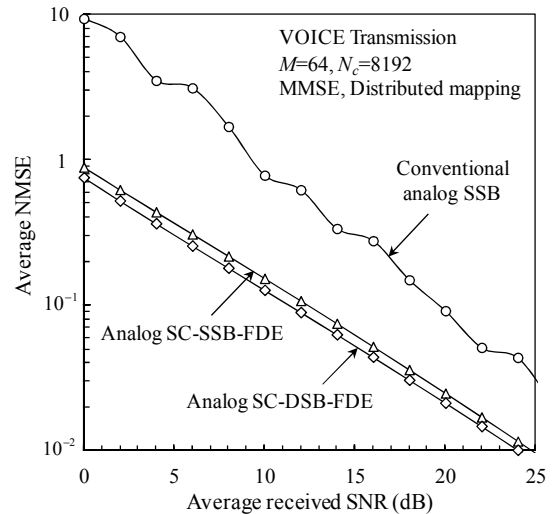


Fig. 4. NMSE performance.

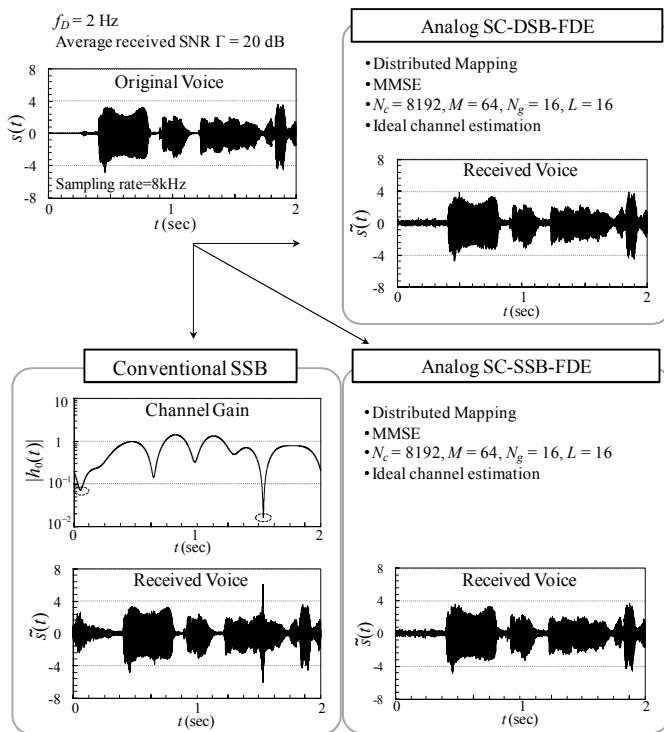


Fig. 5. One-shot observation of voice transmission ($\Gamma = 20$ dB).

Fig. 5 shows a one-shot observation of voice transmission in case of conventional analog SSB and analog SC-SSB-FDE when $\Gamma = 20$ dB. For comparison, the voice transmission of analog SC-DSB-FDE is also observed. The maximum Doppler frequency $f_D = 2$ Hz, ideal channel estimation and fast AGC are assumed. It can be clearly seen that when the channel gain $h(t)$ drops, the noise enhancement appears in the case of conventional analog SSB while the received voice waveform is almost the same as the original waveform in the case of analog SC-SSB-FDE. This is because the combination of MMSE-FDE and distributed mapping not only avoids the noise enhancement but also obtains significant frequency diversity gain. An approximate received voice waveform is also observed between analog SC-DSB-FDE and analog SC-SSB-FDE.

IV. CONCLUSION

In this paper, a novel single sideband transmission technique referred to as analog SC-SSB-FDE was proposed to

double the spectrum efficiency of analog SC-DSB-FDE. In the proposed analog SC-SSB-FDE, after the removal of the frequency components in USB, the resultant frequency components are mapped over a broad bandwidth and FDE is applied to take advantage of the channel frequency-selectivity (i.e., frequency diversity gain). By computer simulation, we showed that analog SC-SSB-FDE, which does not require Hilbert transform, achieves better NMSE performance than conventional analog SSB transmission and keeps the performance quality similar to analog SC-DSB-FDE. In this paper, transmission of single analog signal stream was presented. However, it should be noted that multiple analog signal streams using the proposed analog SC-SSB-FDE can be transmitted based on the FDMA principle with the same spectrum efficiency as the conventional SSB transmission system. The perfect knowledge of channel state information was assumed. Channel estimation for analog SC-SSB-FDE is left as an interesting future study.

REFERENCES

- [1] Y. Kim, B.J. Jeong, J. Chung, C.-S. Hwang, J.S. Ryu, K.-H. Kim, and Y.J. Kim, "Beyond 3G; vision, requirements, and enabling technologies," *IEEE Commun. Mag.*, vol. 41, no. 3, pp. 120-124, March 2003.
- [2] A. Goldsmith, *Wireless communications*, Cambridge University Press, 2005.
- [3] T.H. Vo, S. Kumagai, T. Obara, and F. Adachi, "Analog single-carrier transmission with frequency-domain equalization," *Proc. 19th Asia-Pacific Conference on Communication (APCC 2013)*, pp. 698-702, Aug. 2013.
- [4] A. Czylik, "Comparison between adaptive OFDM and single-carrier modulation with frequency domain equalization," *Proc. IEEE 47th Vehicular Technology Conference*, vol. 2, pp. 865-869, May 1997.
- [5] D. Falconer, S.L. Ariyavistakul, A. Benyamin-Seeyar, and B. Eidson, "Frequency domain equalization for single-carrier broadband wireless systems," *IEEE Commun. Mag.*, vol. 40, no. 4, pp. 58-66, April 2002.
- [6] F. Adachi, H. Tomeba, and K. Takeda, "Frequency-domain equalization for broadband single-carrier multiple access," *IEICE Trans. Commun.*, vol. E92-B, no. 5, pp. 1441-1456, May 2009.
- [7] H.G. Myung, J. Lim, and D.J. Goodman, "Single carrier FDMA for uplink wireless transmission," *IEEE Vehicular Technol. Mag.*, vol. 1, no. 3, pp. 30-38, Sept. 2006.
- [8] Y. Han, Z. Wang, L. Li, and Y. Zhao, "A fast automatic gain control scheme for IEEE 802.15.4 receiver," *Proc. IET 2nd International Conference on Wireless, Mobile and Multimedia Networks (ICWMMN)*, pp. 167-170, Oct. 2008.
- [9] Carl F. Kurth, "Generation of single-sideband signals in multiplex communication systems," *IEEE Trans. on Circuits and Systems*, vol. 23, no. 1, pp. 1-17, Jan. 1976.